

1 **Meteorology, not emissions, helps explain an upward trend in atmospheric methane**
2 **across the US**

3 **Leyang Feng¹, Sakineh Tavakkoli², Sarah M. Jordaan², Arlyn E. Andrews³, Joshua S.**
4 **Benmergui⁴, Darryn W. Waugh⁵, Mingyang Zhang¹, Dylan C. Gaeta¹ and Scot M. Miller¹**

5 ¹Department of Environmental Health and Engineering, Johns Hopkins University, Baltimore,
6 MD

7 ²School of Advanced International Studies, Johns Hopkins University, Washington, DC

8 ³Global Monitoring Laboratory, Earth System Research Laboratories, NOAA, Boulder, CO

9 ⁴John A. Paulson School of Engineering and Applied Sciences, Harvard University, Boston, MA

10 ⁵Department of Earth & Planetary Sciences, Johns Hopkins University, Baltimore, MD

11

12 Corresponding author: Leyang Feng (lfeng13@jhu.edu)

13 **Key Points:**

- 14 • Meteorology helps explain an upward trend in observed atmospheric methane
15 concentrations in the United States between years 2007 and 2015.
- 16 • Trends in local meteorological processes (e.g., annually-averaged horizontal wind speed)
17 correlate with atmospheric methane trends at many locations.
- 18 • This work supports for the conclusion that there was little or no trend in US methane
19 emissions during this time.

20 **Abstract**

21 US natural gas production increased by ~43% between 2005 and 2015, but there is disagreement
22 in the scientific literature on whether this growth led to increased methane emissions. In this
23 study, we evaluate the possible contributions of emissions versus meteorology to an upward
24 trend in US atmospheric methane observations during 2007-2015. We find that interannual
25 variability (IAV) in meteorology yields an apparent upward trend in atmospheric methane across
26 much of the US. We further find that IAV in atmospheric methane at several observation sites is
27 correlated with IAV in local wind speed. Overall, our results show that US trends in atmospheric
28 methane largely reflect variability in meteorology, and are unlikely to be a direct reflection of
29 trends in emissions. The results of this study therefore lend support for the conclusion that there
30 was little upward trend in US methane emissions during this time.

31 **Plain Language Summary**

32 US natural gas production increased from 18 to 27.1 trillion cubic feet per year between 2005
33 and 2015 as a result of the shale gas boom and the associated technological breakthrough of
34 combining horizontal drilling and hydraulic fracturing. This increase in natural gas activity has
35 caused concern about methane emissions, since methane is the primary constituent of natural gas
36 and an important greenhouse gas. However, estimates of trends in US methane emissions have
37 been ambiguous and controversial, and existing studies have reached conflicting conclusions.
38 Furthermore, atmospheric methane levels at many US observation locations have increased faster
39 than the global mean, raising questions about whether increasing US natural gas production has
40 led to increased emissions. In this study, we explore the roles of changing emissions versus
41 changing meteorology in explaining recent increases in atmospheric methane levels across the
42 US. And we find that changing meteorology can explain this recent atmospheric methane
43 increase. The results of this study elucidate the complex relationships between emissions and
44 atmospheric observations and shed light on recent changes in US methane emissions.

45 **1 Introduction**

46 The US is one of the largest anthropogenic emitters of methane, behind only China and
47 India (Saunio et al. 2020). Numerous recent studies indicate that US methane emissions are
48 48% - 76% higher than estimated by the EPA Inventory of US Greenhouse Gas Emissions and
49 Sinks (GHGI) (Alvarez et al. 2018; Barkley et al. 2019, 2021; Caulton et al. 2019; Robertson et
50 al. 2020; Zavala-Araiza et al. 2015). One reason for this discrepancy is that methane emissions
51 are challenging to quantify. For example, recent studies indicate that 5% of oil and gas facilities
52 account for over 50% of emissions (Brandt et al. 2016; see also Omara et al. 2018; Rella et al.
53 2015; Zavala-Araiza et al. 2015, 2017). These facilities can be difficult to find, effectively
54 monitor, and subsequently account for in an emissions inventory that is based upon a limited
55 number of emissions factors.

56 In addition, a marked increase in natural gas activity over the past 15 years has caused
57 concern over possible increases in US methane emissions. US natural gas production increased
58 by 43% between years 2005 and 2015, and this increase is coincident with the deployment of
59 hydraulic fracturing and horizontal drilling technologies (US EIA, 2016). Several studies argue
60 that increased natural gas production activity likely means increased fugitive methane emissions
61 (Howarth et al. 2019). By contrast, EPA's GHGI indicates that total US anthropogenic methane
62 emissions decreased by 5.0% between years 2005 - 2015 and that emissions from the natural gas

63 sector decreased by 8.8% (US EPA, 2021). EPA attributes most of this change in natural gas
64 emissions to decreasing exploration and distribution emissions and reports decreasing emissions
65 factors across many areas of the natural gas sector (US EPA, 2021). These decreasing emissions
66 factors explain why the trend in EPA's emissions inventory is opposite the trend in natural gas
67 production.

68 In addition to the EPA inventory, a handful of studies based on atmospheric observations
69 estimate trends in US methane emissions. However, these studies do not agree on whether US
70 methane emissions increased. Turner et al. (2016) examine trends in atmospheric observations
71 from a site in Oklahoma and from the Greenhouse Gases Observing Satellite (GOSAT). They
72 estimate that US emissions increased by 2.5 - 4.7% per annum between years 2010 and 2014,
73 depending on the observations analyzed. Sheng et al. (2018), also using GOSAT, report a similar
74 upward emissions trend of $2.5 \pm 1.4\%$ per annum between years 2010-2016. By contrast, a
75 handful of additional studies find a much smaller increase or no increase at all. For example, Lan
76 et al. (2019) report a trend in US emissions of $0.7 \pm 0.3\%$ per annum (2006-2015) using in situ
77 observation sites, Maasakkers et al. (2021) estimate a trend of 0.4% per annum (2010-2015)
78 using observations from GOSAT, and Lu et al. (2021) estimate a trend of $0.1 \pm 0.2\%$ per annum
79 (2010-2017) using both GOSAT and in situ observation sites.

80 The purpose of this work is to help reconcile the disparate trends reported by recent
81 studies that use atmospheric methane observations. Specifically, we hypothesize that
82 meteorology produced an upward trend in atmospheric methane across the United States between
83 years 2007-2015, and that this upward trend in meteorology can help explain the disagreement
84 among existing atmospheric estimates of methane emissions trends. To answer this hypothesis,
85 we develop meteorology and emissions trend scenarios to evaluate the plausible impacts of
86 meteorology versus emissions on trends in atmospheric methane levels. In subsequent analyses,
87 we further examine the correlations between inter-annual variability (IAV) in our modeled
88 methane scenarios and IAV in specific meteorological parameters. This analysis sheds light on
89 the specific meteorological processes that correlate with atmospheric methane trends.

90 **2 Data and methods**

91 2.1 Atmospheric modeling

92 We model atmospheric methane mixing ratios (MMR) between years 2007 and 2015 at 8
93 tower measurement sites in the continental US that are part of the National Oceanic and
94 Atmospheric (NOAA) Global Monitoring Laboratory (GML) Cooperative Air Sampling
95 Network (Andrews et al, 2014). Tall tower observations in the US greatly expanded in 2007, and
96 the 8 tower sites included in this study have observations available during all years of the study
97 period. We further model MMR at 80,914 GOSAT sounding locations across the continental US
98 (CONUS) between years 2009 and 2015. GOSAT sounding locations are specifically taken from
99 the UoL Proxy XCH₄ Retrieval Version 9 (Parker et al. 2020). This data product provides total
100 column averaged atmospheric methane mixing ratios at GOSAT sounding locations and is used
101 in several recent studies of methane emissions (Maasakkers et al. 2021; Sheng et al. 2018).

102 We model atmospheric MMR at these locations using simulations from the Stochastic
103 Time-Inverted Lagrangian Transport model (STILT) (e.g., Lin et al. 2003). The simulations used
104 here were generated as part of the NOAA CarbonTracker-Lagrange project (e.g., Hu et al. 2019).

105 STILT is a particle trajectory model; it tracks a large set of tracer particles (500 in this study),
106 and the dispersion of those particles in the atmosphere is used to generate an influence footprint
107 (in the units of atmospheric mixing ratio per unit of emissions). As a result of this setup, we
108 model methane at each location and time by multiplying an individual footprint by a methane
109 emission estimate (described below). Note that the STILT particles are driven by meteorology
110 from the Weather Research and Forecast (WRF) model (Skamarock et al. 2008). To date, WRF-
111 STILT has been used for atmospheric transport in numerous existing regional methane and
112 greenhouse gas modeling studies (Hu et al. 2019; Miller et al. 2013, 2014, 2015; Nehrkorn et al.
113 2010). The WRF simulations have a nested spatial resolution of 10 km over CONUS and 40 km
114 over remaining regions of North America. The STILT footprints are run for a total of 10 days
115 back in time, with a spatial resolution of 1° latitude by 1° longitude.

116 We further use several methane flux estimates to account for multiple different methane
117 source types in the atmospheric modeling simulations. Specifically, we use the US EPA gridded
118 methane emissions inventory across CONUS (Maasakkers et al. 2016) and the Emission
119 Database for Global Atmospheric Research (EDGAR) gridded methane emissions version 5
120 (Crippa et al. 2019) for anthropogenic fluxes outside CONUS. Maasakkers et al. (2021) argue
121 that the EPA inventory underestimates oil and gas emissions but that emissions from other
122 anthropogenic sectors in the US are roughly consistent with atmospheric observations. Hence,
123 we scale US oil production emissions by a factor of 1.59 and gas production emissions by 1.33 to
124 match the inverse modeling estimate of Maasakkers et al. (2021). We additionally use wetland
125 methane fluxes calculated using the model in Pickett-Heaps et al. (2011) (and as used in Miller et
126 al. 2014, 2016). Several atmospheric modeling studies have argued that the wetland flux model
127 from Pickett-Heaps et al. (2011) has a magnitude and spatiotemporal distribution that is
128 generally consistent with in-situ atmospheric methane observations across Canada and the
129 northern US (Miller et al. 2014, 2016; Pickett-Heaps et al. 2011). We further use biomass
130 burning methane fluxes from the Quick Fire Emissions Dataset (QFED v2.4, Darmenov & da
131 Silva, 2013). Maasakkers et al. (2021) find that the overall magnitude of QFED emissions is
132 generally consistent with GOSAT observations. Each of these fluxes are regridded to a 1°
133 latitude by 1° longitude spatial resolution for the atmospheric modeling simulations, though the
134 native spatial resolution of these flux products is higher. Furthermore, anthropogenic and
135 wetland fluxes have a monthly time resolution while QFED has a daily time resolution.

136 2.2 Modeling scenarios and trend fitting

137 We create two emissions scenarios (one with an emissions trend and one without an
138 emissions trend) and two meteorology scenarios (one with IAV in meteorology and one without).
139 In total, we analyze four modeling scenarios: with trends in emissions and IAV in meteorology
140 (scenario 1), with trends in emissions and without IAV in meteorology (scenario 2), no trends in
141 emissions and with IAV in meteorology (scenario 3), and no trends in emissions and without
142 IAV in meteorology (scenario 4).

143 The emissions scenarios are generated based on the methane flux estimates described in
144 Sect. 2.1. For the scenario with no emissions trend, we use the monthly US EPA inventory
145 estimate for year 2012 in all years of the WRF-STILT model simulations. Similarly, we use
146 monthly wetland fluxes and daily QFED fluxes also for year 2012. For the scenario with an
147 emissions trend, we scale oil and gas emissions in each state relative to monthly U.S. dry natural

148 gas production data (US EIA, 2018) from years 2007 to 2015. At the time of writing, emissions
149 from the US EPA gridded inventory are only available for year 2012, and we scale oil and gas
150 emissions up or down relative to 2012 inventory numbers. For the simulations here, we do not
151 add a trend to other methane source types because we are primarily interested in how a plausible
152 trend in oil and gas emissions would manifest at the atmospheric observation sites, all else being
153 constant. Some recent studies argue that US methane emissions trends are likely being driven by
154 the oil and gas sectors (e.g., Sheng et al. 2018, Turner et al. 2016), and we therefore create a
155 hypothetical emissions scenario that focuses on that sector.

156 We further generate meteorology scenarios that include IAV in meteorology and
157 scenarios that do not include IAV in meteorology. For the former scenarios, we run WRF-STILT
158 using standard protocols as described in Sect. 2.1. For the latter scenarios, we average footprints
159 from different years to remove IAV in meteorology. Specifically, at each in-situ monitoring site,
160 we average the footprints from each month of the year across all years of modeling simulations.
161 In other words, we average the WRF-STILT footprints from all Januarys (across 2007-2015),
162 across all Februarys, etc. This approach preserves seasonal variability in the footprints but
163 removes IAV. For the GOSAT observations, we group the observations into 4° latitude by 4°
164 longitude grid boxes across the United States. Within each box, we average the footprints from
165 each month as described above.

166 We subsequently fit trend lines to the model outputs for each scenario. We can then
167 compare and contrast the impact of meteorology versus emissions on apparent trends in MMR.
168 We specifically fit trend lines using the procedures outlined in Lan et al. (2019) for in situ
169 observations and Sheng et al. (2018) for GOSAT observations. We use line-fitting procedures
170 from these studies to ensure that the results presented here are directly comparable to existing
171 research and to ensure that any differences from these existing studies are not due to differences
172 in the trend-fitting procedure. Technical details of trend line fitting can be found in the SI Sect.
173 S1.

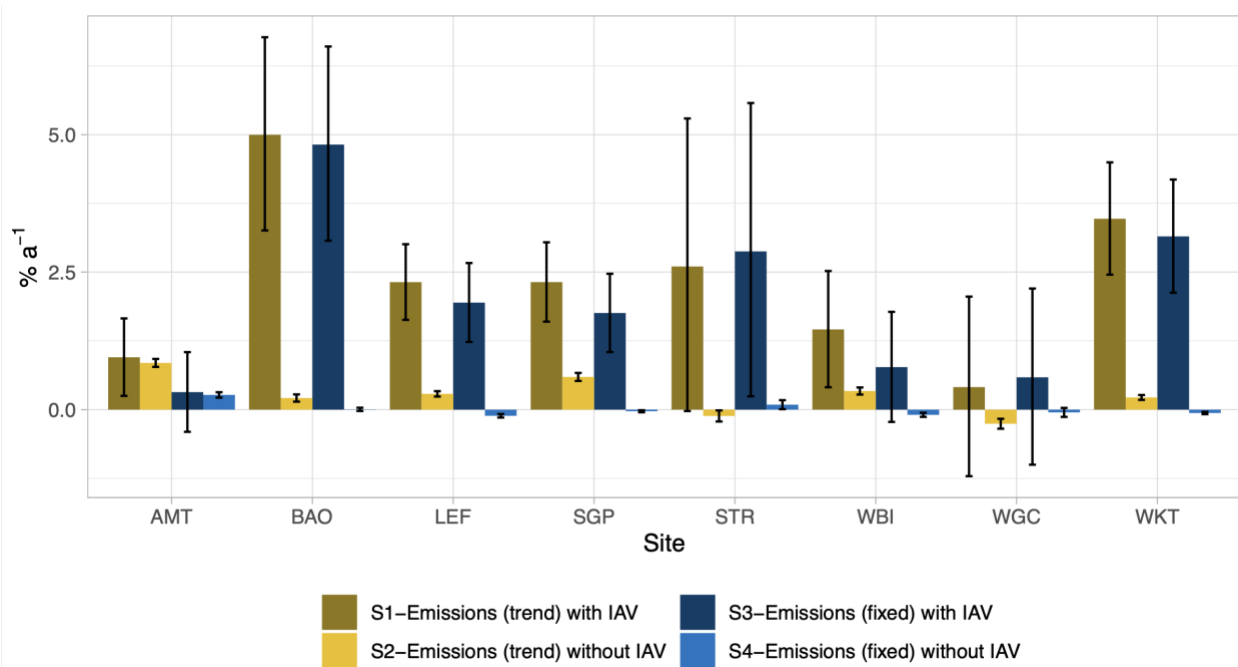
174 **3 Results and discussion**

175 **3.1 Meteorology yields an upward trend in atmospheric methane across the United States**

176 We find that meteorology has a large impact on inter-annual variability (IAV) in modeled
177 methane mixing ratios. For example, we calculate the maximum and minimum values in
178 annually-averaged MMR at each observation site in the NOAA Global Monitoring Laboratory
179 tall tower network. For these calculations, we use anthropogenic emissions that do not contain
180 any trend (e.g., scenario 3 described above), such that IAV in MMR does not reflect variability
181 in emissions. In these simulations, we find, on average, that IAV in MMR at the observation sites
182 is equal to 40% of the total average atmospheric methane signal from North America (Fig. S1 –
183 S8). At some sites, particularly sites that are close to large agricultural or oil and gas emissions
184 sources, this IAV is as high as 59% of the average MMR (e.g., at Eerie, Colorado, site BAO). By
185 contrast, at sites that are distant from large methane emissions, this IAV can be as small as 20%
186 of the average MMR (e.g., at Argyle, Maine, site AMT).

187 In fact, IAV in meteorology also yields an apparent upward trend in MMR at all of the
188 tall tower observation sites. Figure 1 displays the results of the four modeling scenarios at these

189 sites. The individual bars in the plot display the trend (i.e., percent annum change) in MMR at
 190 each observation site estimated using a linear regression (Sect. 2). Specifically, the yellow bars
 191 display the results for scenarios that include a plausible upward trend in emissions while the blue
 192 bars display the results for scenarios that do not include a trend in emissions. Furthermore, dark-
 193 shaded bars display results for scenarios that include IAV in meteorology while light-shaded bars
 194 show scenarios where IAV in meteorology has been removed (Sect. 2). Note that we estimate
 195 negative trends at a few sites in a few scenarios. In most cases, the standard error bars encompass
 196 zero. In two other instances (S2 at STR and WGC), the negative trend estimate occurs at sites
 197 that have a very large seasonal cycle in MMR and have sustained data gaps; the combination
 198 makes trend estimation at these sites prone to error (discussed in Sect. S2).

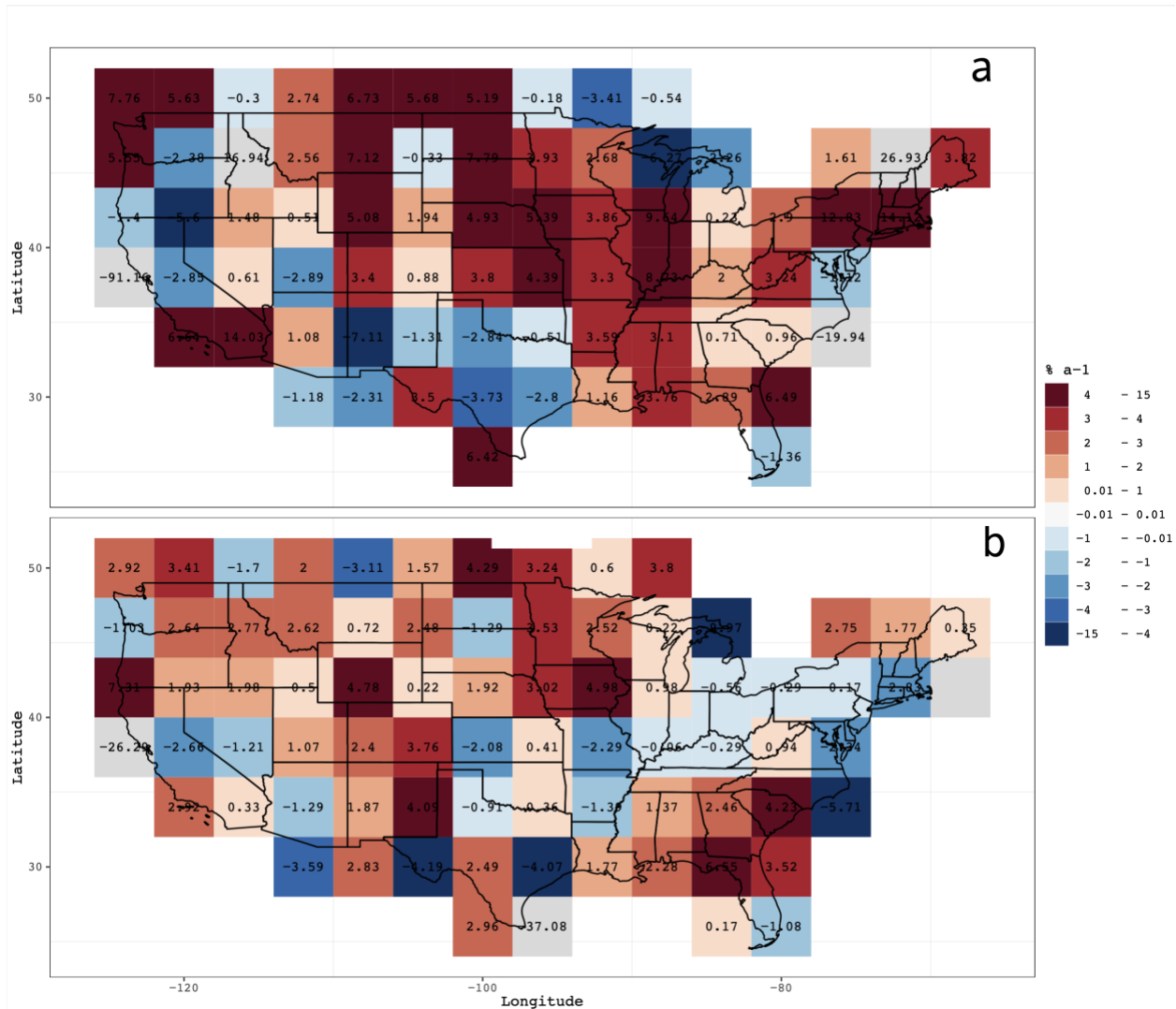


199

200 **Figure 1.** Estimated trends with uncertainty in MMR at different in-situ observation sites (years
 201 2007-2015) and for different modeling scenarios. Sites include Argyle, Maine (AMT); Erie,
 202 Colorado (BAO); Park Falls, Wisconsin (LEF); Billings, Oklahoma (SGP); Sutro Tower, San
 203 Francisco, California (STR); West Branch, Iowa (WBI), Walnut Grove, California (WGC), and
 204 Moody, Texas (WKT) (Andrews et al. 2014). We find that IAV in meteorology has a much
 205 larger impact on estimated trends than does variability in emissions. Note that Figs. S1-S8
 206 display the trends in observed MMR at these sites for reference.

207 We find an upward trend in MMR at all sites, irrespective of whether we include a trend
 208 in emissions (e.g., scenarios S1 and S3). By contrast, when we remove IAV in meteorology, the
 209 upward trend in MMR largely disappears (e.g., scenarios S2 and S4). We therefore conclude that
 210 meteorology is likely driving the trend in model outputs. Furthermore, even when we do not
 211 include a trend in emissions, the trend in the model outputs is often between 2-4% per annum
 212 and ranges from 0.2% per annum (at Argyle) to 5.5% per annum (at Erie) (scenario 3). These
 213 numbers are comparable in magnitude to the US methane emissions trend estimated by several
 214 recent atmospheric studies (e.g., Sheng et al. 2018, Turner et al. 2016). These studies attribute

215 trends in observed atmospheric mixing ratios to emissions, while our results suggest that IAV in
 216 meteorology can yield comparable trends.



217

218 **Figure 2.** Estimated trends in MMR at GOSAT observation sites (years 2009-2015). Panel (a)
 219 displays the result of modeling scenario 3 (IAV in meteorology and no trend in emissions), while
 220 panel (b) displays the estimated trend in GOSAT observations. The modeled trend (a) has a
 221 similar overall magnitude to the observed trend (b), even though the former does not contain an
 222 emissions trend. Note that Fig. S18 – S21 display modeled trends for the three remaining
 223 scenarios not shown here.

224 By contrast, we find that plausible trends in emissions have a smaller impact on estimated
 225 trends in MMR relative to meteorology. For example, scenarios 1 and 3 in Fig. 1 display the
 226 results when we do and do not, respectively, include a plausible trend in anthropogenic
 227 emissions. The differences in estimated trends between these two scenarios is generally small;
 228 the difference is between 0.5 - 1.1% per annum, except at Argyle, a remote site in northern

229 Maine far from large emissions sources. In other words, the impact of an emissions trend is small
230 relative to the overall trend in MMR.

231 Note that we conduct two sensitivity tests for observation sites in oil and gas producing
232 regions (SGP and WKT) – one test that explores the impact of the meteorological product used
233 in STILT and one that explores the impact of observation sampling time and frequency (Figs.
234 S35-36). In simulations using both meteorology products, the impact of a trend in emissions is
235 small relative to IAV due to meteorology, though the models do not always agree on the exact
236 magnitude of MMR in specific months. In the second test, we find that variations in sampling
237 time have little impact on MMR at one site (WKT) but do impact the results at another site
238 (SGP); hence, we cannot rule out the role of observation sampling frequency and time on
239 estimates of atmospheric methane trends.

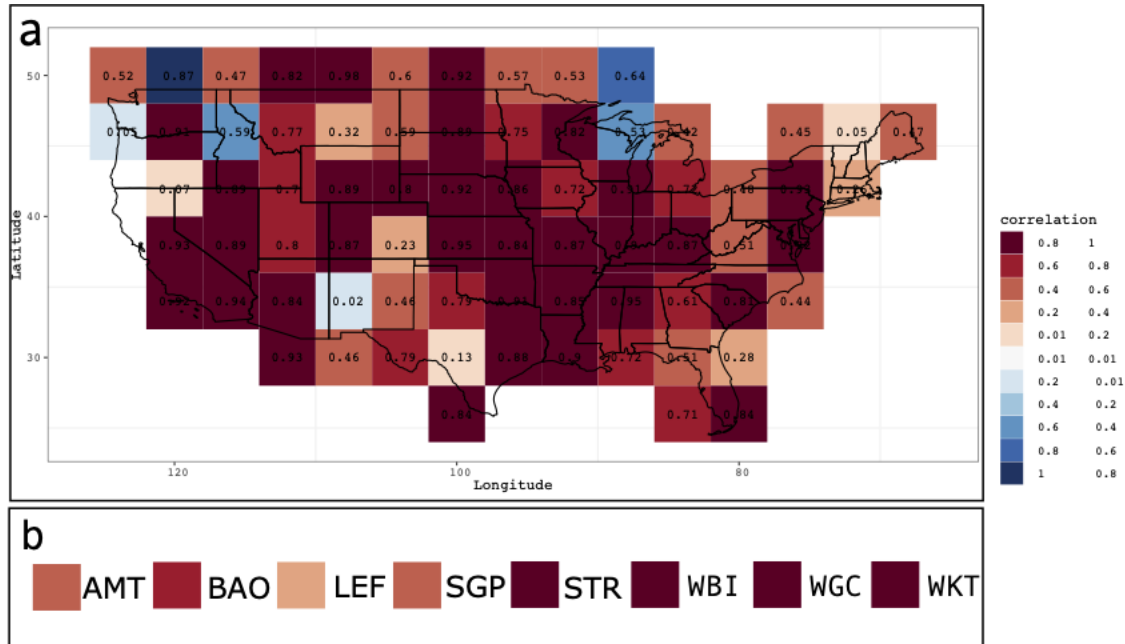
240 We find similar results for simulated GOSAT methane observations. Figure 2 displays
241 the estimated trend in MMR from scenario 3 (panel a) and from the GOSAT observations (panel
242 b) (Fig. S18, S19, and S21 displays scenarios 1, 2, and 4.). The figure shows the trend (% per
243 annum) for model outputs and observations aggregated into 4° by 4° latitude-longitude grid
244 boxes (Sect. 2). The model simulations shown here do not include a trend in emissions, yet the
245 overall trend in MMR is roughly comparable in magnitude to the overall trend in the GOSAT
246 observations. Thus, it is plausible that variability in meteorology is driving much of the observed
247 trend in GOSAT observations. Note that a small number of grid boxes yield unrealistic trend
248 estimates (e.g., coastal northern California and northern Vermont). These grid boxes contain a
249 limited number of observations that are not evenly distributed across seasons and years during
250 the study period, making trend estimation challenging. Also note that Figs. S22-S28 display
251 detailed modeled and observation time series at several prototypical locations across the United
252 States.

253 We note that the results described above could differ if analyzed across a longer time
254 horizon (e.g., across multiple decades). If there were sustained emissions trends across multiple
255 decades, it might be easier to identify directly from atmospheric observations, even given large
256 IAV in meteorology. With that said, existing studies of methane trends have examined similar
257 time periods to this study (e.g., Lan et al. 2019, Maasakkers et al. 2020, Sheng et al. 2018,
258 Turner et al. 2016). Furthermore, observations that span multiple decades are rarely available,
259 except at a handful of global monitoring sites (at the time of writing), and shorter time periods,
260 like those evaluated in this study, are also helpful for evaluating the impacts of emissions
261 policies in a timely manner (e.g., Miller et al. 2019).

262 3.2 Local meteorological processes correlate with atmospheric methane trends

263 In Sect. 3.1, we argue that meteorology yields large IAV in MMR, and a natural follow-
264 up question is to evaluate what specific aspects of meteorology correlate with this IAV. We find
265 that IAV in local meteorological processes show a strong correlation with IAV in MMR. To
266 evaluate this question, we examine the correlation between annually-averaged MMR and the
267 “local” STILT footprint. The STILT footprint estimates the impact of emissions in a given
268 location on the observation site (in units of ppb per unit emission). Here, we define the local
269 footprint as the 1° latitude/longitude grid box where the observation is located, and we then
270 average this footprint across each year. We compare these local footprints against annually-

271 averaged MMR. Figure 3 displays the results of this analysis for model outputs at GOSAT
 272 observation locations (panel a) and in situ observation locations (panel b). We find that the
 273 correlation (r) between MMR and the local footprint is strong -- greater than 0.8 in many
 274 locations for the GOSAT simulations and greater than 0.5 at most locations. The correlation is
 275 similarly strong for the simulations at in situ observation sites -- between 0.8 and 1.0.

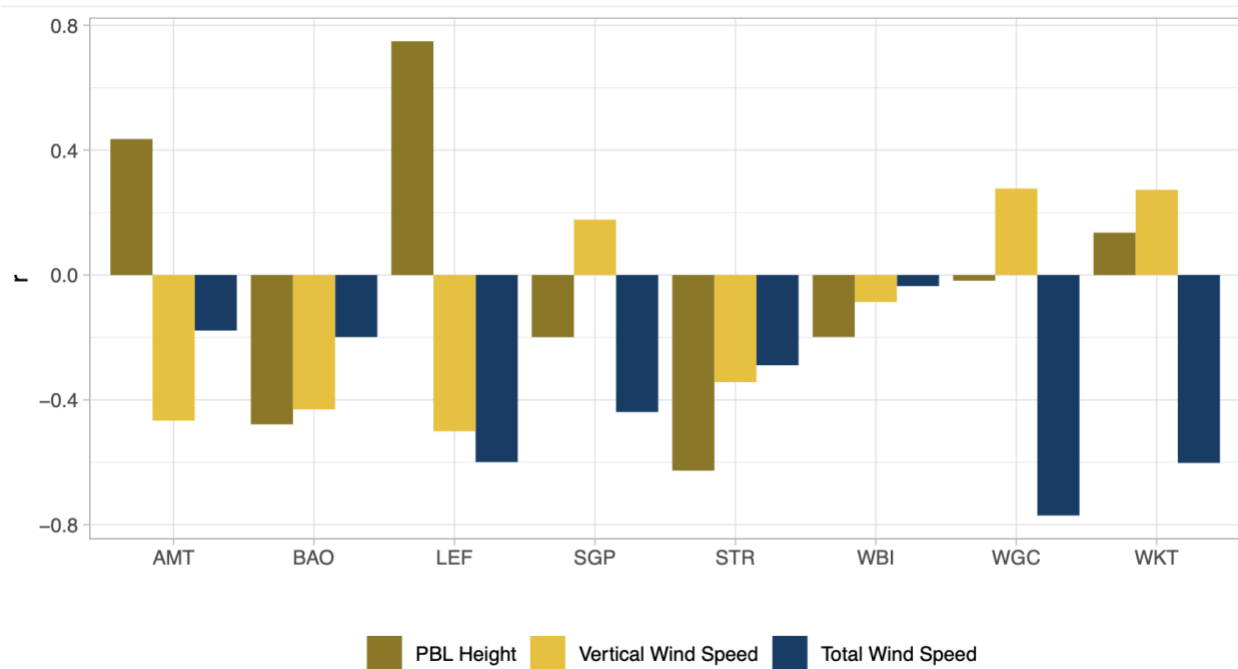


276

277 **Figure 3.** The correlation (r) between annually-averaged MMR and the local footprint (Sect.
 278 3.2), both at GOSAT and in-situ observation locations. We find a close correlation at most
 279 locations, suggesting that local meteorological processes play a key role in IAV of MMR.

280 We further explore the relationships between IAV in MMR and IAV in several specific,
 281 local meteorological processes -- including planetary boundary layer (PBL) height, vertical wind
 282 speed (Ω), and total wind speed at the observation location and modeling height (i.e., the
 283 Euclidean sum of u and v wind speed). In this specific study, we use estimates for these
 284 parameters from North American Regional Reanalysis (NARR, NCEP, 2005). At the in situ
 285 observation sites, we often find the strongest anti-correlations between IAV in MMR and IAV in
 286 annually-averaged local wind speed, particularly at sites near large sources (e.g., WGC and
 287 WKT). When local winds are stagnant, methane (presumably from local sources) accumulates
 288 around the observation site. By contrast, faster winds likely promote greater ventilation and
 289 thereby decrease methane at the observation sites. Urban sites (e.g., STR, BAO), however,
 290 exhibit a stronger anti-correlation with PBL height. At these sites, larger PBL heights are
 291 associated with dilution of the urban pollution dome. Curiously, MMR at two sites (LEF, AMT)

292 is positively correlated with PBL height. At these remote sites, higher PBL heights could be
 293 associated with greater transport of methane from distant source regions.



294

295 **Figure 4.** The correlation (r) between annually-averaged MMR and various meteorological
 296 factors at the in-situ observation sites. We find that MMR is often anti-correlated with local wind
 297 speed, though the strength of that relationship varies by site. By contrast, at urban sites (STR and
 298 BAO), we find the strongest anti-correlation with PBL height.

299 Note that we are not able to identify meaningful correlations between IAV in MMR and
 300 specific meteorological parameters for the GOSAT simulations. GOSAT observes methane
 301 mixing ratios across an entire vertical atmospheric column. As a result, IAV in MMR is likely
 302 influenced by a complex mixture of meteorological parameters across different altitudes.

303 Our findings on methane trends are in parallel with several other studies that report on the
 304 role of atmospheric transport in air pollutant and GHG variability (e.g., Keppel-Aleks et al. 2011,
 305 Kerr et al. 2020, 2021, Samaddar et al. 2021, Torres et al. 2019). These studies generally find
 306 that transport plays a dominant role in explaining meso- and synoptic-scale variability in trace
 307 gas mixing ratios. For example, Keppel-Aleks et al. (2011) report that variations in total column
 308 CO₂ mixing ratios are forced both by local CO₂ fluxes and advection on diurnal scales, and on
 309 synoptic scales, CO₂ variations arise due to large-scale eddy-driven disturbances of the
 310 meridional gradient. Torres et al. (2019) report similar findings using CO₂ observations from the
 311 Orbiting Carbon Observatory 2 (OCO-2). Kerr et al. (2020, 2021) further argue that daily,
 312 continental-scale variations of O₃ are largely meteorology driven and are influenced by the
 313 meridional flow related to the jet stream. In the present study, we also find that transport plays a

314 dominant role in trace gas (i.e., CH₄) mixing ratios, albeit at annual instead of the daily/synoptic
315 scales examined in the aforementioned studies.

316 **4 Conclusions**

317 Natural gas production activities in the US increased during the shale gas boom, leading
318 to concerns about increasing methane emissions. In fact, several studies report increasing MMR
319 across the US relative to the global mean. However, we find that meteorology, not emissions,
320 can explain this upward trend MMR between 2007 and 2015. We then explore which
321 meteorological factors correlate with this upward trend. Using a footprint analysis, we argue that
322 IAV in MMR is likely correlated with local meteorological processes. At in situ monitoring sites,
323 we also find higher correlations between MMR and IAV in local wind speed than with
324 meteorological parameters related to vertical mixing.

325 Overall, our results show that IAV in MMR reflect variability in meteorology as much or
326 more than variability in emissions. This finding poses an inherent challenge for detecting trends
327 in emissions because, at least in the case of methane, the atmospheric signal of that emissions
328 trend is comparatively small. This result is especially applicable given the limited time span of
329 many existing in situ and satellite observation records. This study further cautions against
330 interpreting trends in atmospheric greenhouse gas mixing ratios as a direct proxy for trends in
331 emissions.

332 This work also lends support for existing studies that show little or no trend in US
333 methane emissions. Specifically, existing studies fall into two categories: studies that directly
334 interpret trends in atmospheric observations (e.g., Lan et al. 2019, Sheng et al. 2018, Turner et al.
335 2016) and studies that estimate emissions using inverse modeling, which accounts for
336 meteorology using a modeled and/or reanalysis product (e.g., Benmergui et al. 2015, Lu et al.
337 2021, Maasakers et al. 2020). Studies that directly interpret trends from atmospheric
338 observations find an upward emissions trend during a similar time period as the present study
339 (2.5 - 4.7% per annum). By contrast, studies that account for atmospheric transport through the
340 use of inverse modeling find little upward trend in methane emissions (e.g., 0.1 - 0.7% per
341 annum). Inverse modeling studies account for trends in MMR due to meteorology instead of
342 aliasing the trends on emissions, and the present studies therefore helps explain these seemingly
343 irreconcilable results.

344 **Acknowledgments**

345 This work was funded by a Johns Hopkins University Discovery Grants. The authors declare no
346 conflicts of interest. We thank Thomas Nehrkorn and Marikate Mountain from AER, Inc. for
347 generating STILT footprints.

349 **Open Research**

350 The in situ observations used in this study are available from the NOAA Global Monitoring
351 Laboratory ObsPack (Cooperative Global Atmospheric Data Integration Project 2020). The
352 GOSAT methane observations (UoL Proxy XCH₄ Retrieval Version 9) are available at
353 <http://dx.doi.org/10.5285/18ef8247f52a4cb6a14013f8235cc1eb>. In addition, STILT footprints
354 from CarbonTracker-Lagrange are available at <https://gml.noaa.gov/ccgg/carbontracker-lagrange/>.

356
357
358
359
360
361
362
363
364
365
366
367
368
369
370
371
372
373
374
375
376
377
378
379
380
381
382
383
384
385
386
387
388
389
390
391
392
393
394
395
396
397
398
399
400

References

- Andrews, A. E., Kofler, J. D., Trudeau, M. E., Williams, J. C., Neff, D. H., Masarie, K. A., et al. (2014). CO₂, CO, and CH₄ measurements from tall towers in the NOAA Earth System Research Laboratory's Global Greenhouse Gas Reference Network: Instrumentation, uncertainty analysis, and recommendations for future high-accuracy greenhouse gas monitoring efforts. *Atmospheric Measurement Techniques*, 7(2), 647-687. <https://doi.org/10.5194/amt-7-647-2014>
- Alvarez, R. A., Zavala-Araiza, D., Lyon, D. R., Allen, D. T., Barkley, Z. R., Brandt, A. R., et al. (2018). Assessment of methane emissions from the US oil and gas supply chain. *Science*, 361(6398), 186-188. <https://doi.org/10.1126/science.aar7204>
- Barkley, Z. R., Davis, K. J., Feng, S., Cui, Y. Y., Fried, A. L. A. N., Weibring, P. E. T. T. E. R., et al. (2021). Analysis of Oil and Gas Ethane and Methane Emissions in the Southcentral and Eastern United States Using Four Seasons of Continuous Aircraft Ethane Measurements. *Journal of Geophysical Research: Atmospheres*, 126(10), e2020JD034194. <https://doi.org/10.1029/2020JD034194>
- Barkley, Z. R., Lauvaux, T., Davis, K. J., Deng, A., Fried, A., Weibring, P., et al. (2019). Estimating methane emissions from underground coal and natural gas production in Southwestern Pennsylvania. *Geophysical Research Letters*, 46(8), 4531-4540. <https://doi.org/10.1029/2019GL082131>
- Benmergui, J. S., Andrews, A. E., Thoning, K. W., Trudeau, M., Miller, S. M., Dlugokencky, E. J., et al. (2015). Integrating diverse observations of North American CH₄ into flux inversions in CarbonTrackerLagrange-CH₄. In *AGU Fall Meeting Abstracts* (Vol. 2015, pp. A33F-0245).
- Brandt, A. R., Heath, G. A., & Cooley, D. (2016). Methane Leaks from Natural Gas Systems Follow Extreme Distributions. *Environmental Science & Technology*, 50(22), 12512-12520. <https://doi.org/10.1021/acs.est.6b04303>
- Caulton, D. R., Lu, J. M., Lane, H. M., Buchholz, B., Fitts, J. P., Golston, L. M., et al. (2019). Importance of Superemitter Natural Gas Well Pads in the Marcellus Shale. *Environmental Science & Technology*, 53(9), 4747-4754. <https://doi.org/10.1021/acs.est.8b06965>
- Cleveland, R. B., Cleveland, W. S., and Terpenning, I.: STL: A seasonal-trend Decomposition Procedure Based on Loess, *Journal of Official Statistics*, 6, 3-73, 1990.
- Crippa, M., Oreggioni, G., Guizzardi, D., Muntean, M., Schaaf, E., Lo Vullo, E., et al. (2019). Fossil CO₂ and GHG emissions of all world countries - 2019 Report, *EUR 29849 EN*, Publications Office of the European Union, Luxembourg, 2019, ISBN 978-92-76-11100-9, <https://doi.org/10.2760/687800>
- Cooperative Global Atmospheric Data Integration Project; (2020): Multi-laboratory compilation of atmospheric methane data for the period 1957-2018;

- 401 obspack_ch4_1_GLOBALVIEWplus_v2.0_2020-04-24 [Dataset]; NOAA Earth System
402 Research Laboratory, Global Monitoring Division. <http://dx.doi.org/10.25925/20200424>
403
- 404 Cui, Y. Y., Brioude, J., Angevine, W. M., Peischl, J., McKeen, S. A., Kim, S. W., et al. (2017).
405 Top-down estimate of methane emissions in California using a mesoscale inverse modeling
406 technique: The San Joaquin Valley. *Journal of Geophysical Research: Atmospheres*, 122(6),
407 3686-3699. <https://doi.org/10.1002/2016JD026398>
408
- 409 Cui, Y. Y., Brioude, J., McKeen, S. A., Angevine, W. M., Kim, S. W., Frost, G. J., et al. (2015).
410 Top-down estimate of methane emissions in California using a mesoscale inverse modeling
411 technique: The South Coast Air Basin. *Journal of Geophysical Research: Atmospheres*, 120(13),
412 6698-6711. <https://doi.org/10.1002/2014JD023002>
413
- 414 Darmenov, A. & da Silva, A. (2013). *The quick fire emissions dataset (QFED)—documentation of*
415 *versions 2.1, 2.2 and 2.4, NASA Technical Report Series on Global Modeling and Data*
416 *Assimilation, NASA TM-2013-104606*. (Vol. 38).
417 <https://ntrs.nasa.gov/api/citations/20180005253/downloads/20180005253.pdf>
418
- 419 Goldstein, A. H., Wofsy, S. C., & Spivakovsky, C. M. (1995). Seasonal variations of
420 nonmethane hydrocarbons in rural New England: Constraints on OH concentrations in northern
421 midlatitudes. *Journal of Geophysical Research: Atmospheres*, 100(D10), 21023-21033.
422 <https://doi.org/10.1029/95JD02034>
423
- 424 Howarth, R. W. (2019). Ideas and perspectives: is shale gas a major driver of recent increase in
425 global atmospheric methane?. *Biogeosciences*, 16(15), 3033-3046. [https://doi.org/10.5194/bg-16-](https://doi.org/10.5194/bg-16-3033-2019)
426 [3033-2019](https://doi.org/10.5194/bg-16-3033-2019)
427
- 428 Hu, L., Andrews, A. E., Thoning, K. W., Sweeney, C., Miller, J. B., Michalak, A. M., et al.
429 (2019). Enhanced North American carbon uptake associated with El Niño. *Science Advances*,
430 5(6), eaaw0076. <https://doi.org/10.1126/sciadv.aaw0076>
431
- 432 Huang, Y., Kort, E. A., Gourdji, S., Karion, A., Mueller, K., & Ware, J. (2019). Seasonally
433 resolved excess urban methane emissions from the Baltimore/Washington, DC metropolitan
434 region. *Environmental Science & Technology*, 53(19), 11285-11293.
435 <https://doi.org/10.1021/acs.est.9b02782>
436
- 437 Jeong, S., Hsu, Y. K., Andrews, A. E., Bianco, L., Vaca, P., Wilczak, J. M., et al. (2013). A
438 multitower measurement network estimate of California's methane emissions. *Journal of*
439 *Geophysical Research: Atmospheres*, 118(19), 11-339. <https://doi.org/10.1002/jgrd.50854>
440
- 441 Keppel-Aleks, G., Wennberg, P. O., & Schneider, T. (2011). Sources of variations in total
442 column carbon dioxide. *Atmospheric Chemistry and Physics*, 11(8), 3581-3593.
443 <https://doi.org/10.5194/acp-11-3581-2011>
444

- 445 Kerr, G. H., Waugh, D. W., & Miller, S. M. (2021). Jet Stream-Surface Tracer Relationships:
446 Mechanism and Sensitivity to Source Region. *Geophysical Research Letters*, 48(1),
447 e2020GL090714. <https://doi.org/10.1029/2020GL090714>
448
- 449 Kerr, G. H., Waugh, D. W., Steenrod, S. D., Strode, S. A., & Strahan, S. E. (2020). Surface
450 Ozone-Meteorology Relationships: Spatial Variations and the Role of the Jet Stream. *Journal of*
451 *Geophysical Research: Atmospheres*, 125(21), e2020JD032735.
452 <https://doi.org/10.1029/2020JD032735>
453
- 454 Lan, X., Tans, P., Sweeney, C., Andrews, A., Dlugokencky, E., Schwietzke, S., et al. (2019).
455 Long-term measurements show little evidence for large increases in total US methane emissions
456 over the past decade. *Geophysical Research Letters*, 46(9), 4991-4999.
457 <https://doi.org/10.1029/2018GL081731>
458
- 459 Lin, J. C., Gerbig, C., Wofsy, S. C., Andrews, A. E., Daube, B. C., Davis, K. J., et al. (2003). A
460 near-field tool for simulating the upstream influence of atmospheric observations: The Stochastic
461 Time-Inverted Lagrangian Transport (STILT) model. *Journal of Geophysical Research:*
462 *Atmospheres*, 108(D16). <https://doi.org/10.1029/2002JD003161>
463
- 464 Lu, X., Jacob, D. J., Wang, H., Maasackers, J. D., Zhang, Y., Scarpelli, T. R., et al. (2021).
465 Methane emissions in the United States, Canada, and Mexico: Evaluation of national methane
466 emission inventories and sectoral trends by inverse analysis of in situ (GLOBALVIEWplus CH₄
467 ObsPack) and satellite (GOSAT) atmospheric observations. *Atmospheric Chemistry and Physics*
468 *Discussions*, 1-41. <https://doi.org/10.5194/acp-22-395-2022>
469
- 470 Maasackers, J. D., Jacob, D. J., Sulprizio, M. P., Scarpelli, T. R., Nesser, H., Sheng, J., et al.
471 (2021). 2010–2015 North American methane emissions, sectoral contributions, and trends: a
472 high-resolution inversion of GOSAT observations of atmospheric methane. *Atmospheric*
473 *Chemistry and Physics*, 21(6), 4339-4356. <https://doi.org/10.5194/acp-21-4339-2021>
474
- 475 Maasackers, J. D., Jacob, D. J., Sulprizio, M. P., Turner, A. J., Weitz, M., Wirth, T., et al.
476 (2016). Gridded national inventory of US methane emissions. *Environmental Science &*
477 *Technology*, 50(23), 13123-13133. <https://doi.org/10.1021/acs.est.6b02878>
478
- 479 Miller, S. M., Andrews, A. E., Benmergui, J., Commane, R., Dlugokencky, E. J., Janssens-
480 Maenhout, G., et al. (2015). The ability of atmospheric data to resolve discrepancies in wetland
481 methane estimates over North America. *Biogeosciences Discussions*, 12(23).
482 <https://doi.org/10.5194/bgd-12-9341-2015>
483
- 484 Miller, S. M., Commane, R., Melton, J. R., Andrews, A. E., Benmergui, J., Dlugokencky, E. J.,
485 et al. (2016). Evaluation of wetland methane emissions across North America using atmospheric
486 data and inverse modeling. *Biogeosciences*, 13(4), 1329-1339. [https://doi.org/10.5194/bg-13-](https://doi.org/10.5194/bg-13-1329-2016)
487 1329-2016
488

- 489 Miller, S. M., Michalak, A. M., Detmers, R. G., Hasekamp, O. P., Bruhwiler, L. M., &
490 Schwietzke, S. (2019). China's coal mine methane regulations have not curbed growing
491 emissions. *Nature Communications*, *10*(1), 1-8. <https://doi.org/10.1038/s41467-018-07891-7>
492
- 493 Miller, S. M., Miller, C. E., Commane, R., Chang, R. Y. W., Dinardo, S. J., Henderson, J. M., et
494 al. (2016). A multiyear estimate of methane fluxes in Alaska from CARVE atmospheric
495 observations. *Global Biogeochemical Cycles*, *30*(10), 1441-1453.
496 <https://doi.org/10.1002/2016GB005419>
497
- 498 Miller, S. M., Wofsy, S. C., Michalak, A. M., Kort, E. A., Andrews, A. E., Biraud, S. C., et al.
499 (2013). Anthropogenic emissions of methane in the United States. *Proceedings of the National*
500 *Academy of Sciences*, *110*(50), 20018-20022. <https://doi.org/10.1073/pnas.1314392110>
501
- 502 Miller, S. M., Worthy, D. E., Michalak, A. M., Wofsy, S. C., Kort, E. A., Havice, T. C., et al.
503 (2014). Observational constraints on the distribution, seasonality, and environmental predictors
504 of North American boreal methane emissions. *Global Biogeochemical Cycles*, *28*(2), 146-160.
505 <https://doi.org/10.1002/2013GB004580>
506
- 507 Nehr Korn, T., Eluszkiewicz, J., Wofsy, S. C., Lin, J. C., Gerbig, C., Longo, M., et al. (2010).
508 Coupled weather research and forecasting—stochastic time-inverted lagrangian transport (WRF–
509 STILT) model. *Meteorology and Atmospheric Physics*, *107*(1), 51-64.
510 <https://doi.org/10.1007/s00703-010-0068-x>
511
- 512 National Centers for Environmental Prediction/National Weather Service/NOAA/U.S.
513 Department of Commerce. (2005). NCEP North American Regional Reanalysis (NARR)
514 [Dataset]. Research Data Archive at the National Center for Atmospheric Research,
515 Computational and Information Systems Laboratory. <https://rda.ucar.edu/datasets/ds608.0>
516
- 517 National Centers for Environmental Prediction/National Weather Service/NOAA/U.S.
518 Department of Commerce, (2015): NCEP North American Mesoscale (NAM) 12 km Analysis
519 [Dataset]. Research Data Archive at the National Center for Atmospheric Research,
520 Computational and Information Systems Laboratory, Boulder, CO.
521 <https://doi.org/10.5065/G4RC-1N91>
522
- 523 Omara, M., Zimmerman, N., Sullivan, M. R., Li, X., Ellis, A., Cesa, R., et al. (2018). Methane
524 emissions from natural gas production sites in the United States: Data synthesis and national
525 estimate. *Environmental Science & Technology*, *52*(21), 12915-12925.
526 <https://doi.org/10.1021/acs.est.8b03535>
527
- 528 Parker, R. J., Webb, A., Boesch, H., Somkuti, P., Barrio Guillo, R., Di Noia, A., et al. (2020). A
529 decade of GOSAT Proxy satellite CH₄ observations, *Earth System Science Data*, *12*, 3383–3412.
530 <https://doi.org/10.5194/essd-12-3383-2020>, 2020
531
- 532 Pickett-Heaps, C. A., Jacob, D. J., Wecht, K. J., Kort, E. A., Wofsy, S. C., Diskin, G. S., et al.
533 (2011). Magnitude and seasonality of wetland methane emissions from the Hudson Bay

- 534 Lowlands (Canada). *Atmospheric Chemistry and Physics*, 11(8), 3773-3779.
535 <https://doi.org/10.5194/acp-11-3773-2011>
536
- 537 Rella, C. W., Tsai, T. R., Botkin, C. G., Crosson, E. R., & Steele, D. (2015). Measuring
538 emissions from oil and natural gas well pads using the mobile flux plane technique.
539 *Environmental Science & Technology*, 49(7), 4742-4748.
540 <https://doi.org/10.1021/acs.est.5b00099>
541
- 542 Ren, X., Salmon, O. E., Hansford, J. R., Ahn, D., Hall, D., Benish, S. E., et al. (2018). Methane
543 emissions from the Baltimore-Washington area based on airborne observations: Comparison to
544 emissions inventories. *Journal of Geophysical Research: Atmospheres*, 123(16), 8869-8882.
545 <https://doi.org/10.1029/2018JD028851>
546
- 547 Robertson, A. M., Edie, R., Field, R. A., Lyon, D., McVay, R., Omara, M., et al. (2020). New
548 Mexico Permian Basin measured well pad methane emissions are a factor of 5–9 times higher
549 than US EPA estimates. *Environmental Science & Technology*, 54(21), 13926-13934.
550 <https://doi.org/10.1021/acs.est.0c02927>
551
- 552 Samaddar, A., Feng, S., Lauvaux, T., Barkley, Z. R., Pal, S., & Davis, K. J. (2021). Carbon
553 dioxide distribution, origins, and transport along a frontal boundary during summer in mid-
554 latitudes. *Journal of Geophysical Research: Atmospheres*, 126(9), e2020JD033118.
555 <https://doi.org/10.1029/2020JD033118>
556
- 557 Saunio, M., Stavert, A. R., Poulter, B., Bousquet, P., Canadell, J. G., Jackson, R. B., et al.
558 (2020). The global methane budget 2000–2017. *Earth System Science Data*, 12(3), 1561-1623.
559 <https://doi.org/10.5194/essd-12-1561-2020>
560
- 561 Sargent, M. R., Floerchinger, C., McKain, K., Budney, J., Gottlieb, E. W., Hutyra, L. R., et al.
562 (2021). Majority of US urban natural gas emissions unaccounted for in inventories. *Proceedings*
563 *of the National Academy of Sciences*, 118(44). <https://doi.org/10.1073/pnas.2105804118>
564
- 565 Sheng, J. X., Jacob, D. J., Turner, A. J., Maasakkers, J. D., Benmergui, J., Bloom, A. A., et al.
566 (2018). 2010–2016 methane trends over Canada, the United States, and Mexico observed by the
567 GOSAT satellite: contributions from different source sectors. *Atmospheric Chemistry and*
568 *Physics*, 18(16), 12257-12267. <https://doi.org/10.5194/acp-18-12257-2018>
569
- 570 Shiga, Y. P., Michalak, A. M., Fang, Y., Schaefer, K., Andrews, A. E., Huntzinger, D. H., et al.
571 (2018). Forests dominate the interannual variability of the North American carbon sink.
572 *Environmental Research Letters*, 13(8), 084015. <http://dx.doi.org/10.1088/1748-9326/aad505>
573
- 574 Shiga, Y. P., Tadić, J. M., Qiu, X., Yadav, V., Andrews, A. E., Berry, J. A., et al. (2018).
575 Atmospheric CO₂ observations reveal strong correlation between regional net biospheric carbon
576 uptake and solar-induced chlorophyll fluorescence. *Geophysical Research Letters*, 45(2), 1122-
577 1132. <https://doi.org/10.1002/2017GL076630>
578

- 579 Skamarock, W. C., Klemp, J. B., Dudhia, J., Gill, D. O., Barker, D. M., Wang, W., et al. (2008).
580 A description of the Advanced Research WRF version 3. *NCAR Technical note-475+ STR*.
581 <https://doi.org/10.5065/D68S4MVH>
582
- 583 Torres, A. D., Keppel-Aleks, G., Doney, S. C., Fendrock, M., Luis, K., & Wunch, D. (2019). A
584 geostatistical framework for quantifying the imprint of mesoscale atmospheric transport on
585 satellite trace gas retrievals. *Journal of Geophysical Research: Atmospheres*, 124(17-18), 9773-
586 9795. <https://doi.org/10.1029/2018JD029933>
587
- 588 Turner, A. J., Jacob, D. J., Benmergui, J., Wofsy, S. C., Maasackers, J. D., Butz, A., et al.
589 (2016). A large increase in US methane emissions over the past decade inferred from satellite
590 data and surface observations. *Geophysical Research Letters*, 43(5), 2218-2224.
591 <https://doi.org/10.1002/2016GL067987>
592
- 593 United States Energy Information Administration (2016). Hydraulically fractured wells provide
594 two-thirds of U.S. natural gas production.
595 <https://www.eia.gov/todayinenergy/detail.php?id=26112>
596
- 597 United States Energy Information Administration. (2018). Natural Gas Gross Withdrawals and
598 Production [Dataset]. https://www.eia.gov/dnav/ng/ng_prod_sum_a_EPG0_FPD_mmc_f_m.htm
599
- 600 United States Environmental Protection Agency (2021). Inventory of U.S. greenhouse gas
601 emissions and sink. [https://www.epa.gov/sites/default/files/2021-04/documents/us-ghg-
602 inventory-2021-main-text.pdf?VersionId=yu89kg1O2qP754CdR8Qmyn4RRWc5iodZ](https://www.epa.gov/sites/default/files/2021-04/documents/us-ghg-inventory-2021-main-text.pdf?VersionId=yu89kg1O2qP754CdR8Qmyn4RRWc5iodZ)
603
- 604 Zavala-Araiza, D., Alvarez, R. A., Lyon, D. R., Allen, D. T., Marchese, A. J., Zimmerle, D. J., et
605 al. (2017). Super-emitters in natural gas infrastructure are caused by abnormal process
606 conditions. *Nature Communications*, 8(1), 1-10. <https://doi.org/10.1038/ncomms14012>
607
- 608 Zavala-Araiza, D., Lyon, D. R., Alvarez, R. A., Davis, K. J., Harriss, R., Herndon, S. C., et al.
609 (2015). Reconciling divergent estimates of oil and gas methane emissions. *Proceedings of the
610 National Academy of Sciences*, 112(51), 15597-15602. <https://doi.org/10.1073/pnas.1522126112>